Journal of Power Sources 211 (2012) 103–107

Contents lists available at SciVerse ScienceDirect

Journal of Power Sources

journal homepage: www.elsevier.com/locate/jpowsour

Short communication

High-performing Sn–Co nanowire electrodes as anodes for lithium-ion batteries

Germano Ferrara [a], Catia Arbizzani [b], Libero Damen [b], Martina Guidotti [b], Mariachiara Lazzari [b], Francesco Gioacchino Vergottini [c], Rosalinda Inguanta [c], Salvatore Piazza [c], Carmelo Sunseri [c], Marina Mastragostino [b,*]

[a] CR Mobility Solution System S.r.l., Via Torrearsa 24, 90139 Palermo, Italy
[b] Università degli Studi di Bologna, Dipartimento di Scienza dei Metalli, Elettrochimica e Tecniche Chimiche, Via San Donato 15, 40127 Bologna, Italy
[c] Università di Palermo, Dipartimento di Ingegneria Chimica, Gestionale, Informatica, Meccanica, Viale delle Scienze Ed. 6, 90128 Palermo, Italy

ARTICLE INFO

Article history:
Received 23 January 2012
Received in revised form
7 March 2012
Accepted 21 March 2012
Available online 10 April 2012

Keywords:
Tin
Tin–cobalt alloy
Nanowire
Anode
Vinylene carbonate additive
Li-ion batteries

ABSTRACT

The preparation of Sn_2Co_3 nanowire arrays (NWs) electrogrown inside the channels of polycarbonate membranes and their characterization as anodes for Li-ion batteries both in half-cell *vs.* Li and in battery configuration are reported. The Sn_2Co_3 NW electrodes tested by deep galvanostatic charge/discharge cycles in ethylene carbonate-dimethylcarbonate (1:1) – $LiPF_6$ 1 M displayed 80% capacity retention after 200 cycles at C/2 and 30 °C, and a high charge and discharge rate capability at C-rate from C/3 (0.33 A/g) to 10C (10 A/g) at 30° and 10 °C. Electrodes with the highest alloy loading delivered up to 0.6 mAh cm^{-2} at C/2.

The performance of these electrodes in battery configuration with $LiFePO_4$ as cathode is also reported, as well as the effect of the vinylene carbonate additive on the charge/discharge coulombic efficiency of the Sn_2Co_3 NWs.

1. Introduction

Nanoarchitectures such as nanowires (NWs) are a breakthrough in electrode configuration for next-generation rechargeable lithium-ion batteries, which are the main energy storage systems. In an effort to enhance energy and power, attention has been given to Sn for its high theoretical specific capacity (993 mAh g^{-1}) as an alternative anode to graphite. However, upon lithium insertion/deinsertion tin undergoes a large volume change that induces electrode pulverization with a dramatic capacity fade over cycling; nanometric materials and binary (Sn-inactive metal) alloys have been the main strategies to reduces this drawback [1,2]. After Li and Martin [3], NW technology combined with such intermetallic compounds as Co–Sn, Cu–Sn, and Ni–Sn has several advantages: the space among NWs accommodates volume expansion during Li insertion, whereas the inactive matrix limits volume expansion; electrolyte access is easy and the high electrode/electrolyte contact area leads to high charge/discharge rates. Furthermore, NWs are independently connected to the current collector and, hence, do not need binder or conductive additives [4–9].

We report the electrochemical preparation of Sn–Co nanowires inside the channels of polycarbonate membranes with a higher Co content than those in Ref. [5] to increase the inactive matrix "buffering" effect and, thus, the cycling stability of the electrodes. The electrochemical performance of these Sn–Co NW electrodes in ethylene carbonate (EC) – dimethylcarbonate (DMC) 1:1 – $LiPF_6$ 1 M *vs.* Li and in battery configuration with $LiFePO_4$ as cathode are reported and discussed. The effect of the vinylene carbonate additive on the charge/discharge coulombic efficiency of the Sn–Co NWs is also reported.

2. Experimental

2.1. Preparation of Sn–Co NWs

We have prepared tin-cobalt NWs by electrodeposition inside the nanometric pores of commercially available track-etched polycarbonate membranes (Whatman Cyclopore™, ca. 4.7 cm diameter, ca. 20 μm thickness, nominal pore diameter of 200 nm, and pore density of 10^{12} m^{-2}). First a gold film of 9 μg cm^{-2} was sputtered on one side of the membrane to make it conductive, this side was then glued by a conductive paste to a suitable holder for deposition of the Cu current collector and, subsequently, the Sn–Co

* Corresponding author. Tel.: +39 051 2099798; fax: +39 051 2099365.
E-mail address: marina.mastragostino@unibo.it (M. Mastragostino).

0378-7753/$ – see front matter © 2012 Elsevier B.V. All rights reserved.
doi:10.1016/j.jpowsour.2012.03.066

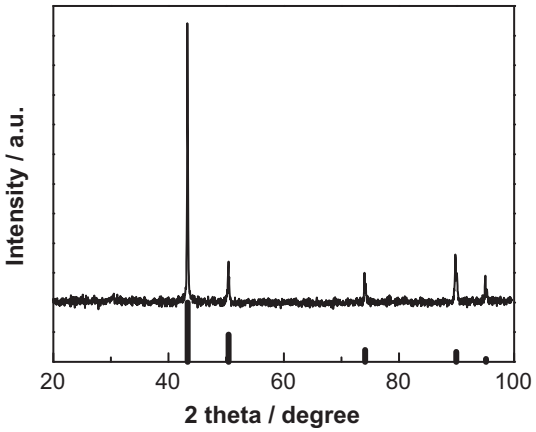

Fig. 1. XRD pattern of the electrodeposited Sn–Co NWs after template polycarbonate membrane dissolution.

alloy NWs were electrodeposited. The Sn–Co NW deposition was performed under potentiostatic conditions at −1.30 V *vs.* SCE by a 273A EG&G Potentiostat/Galvanostat in a three-electrode cell (Pt wire as counter and SCE as reference electrode) in an aqueous electrolytic bath of composition $SnSO_4$ and $CoSO_4$ 0.01 mol L^{-1}, and Na_2SO_4 and sodium gluconate ($C_6H_{11}O_7Na$) 0.2 mol L^{-1}. The polycarbonate membrane was dissolved in trichloromethane and the resulting Sn–Co NW architecture on copper current collector was a ready-to-use electrode for lithium-ion batteries.

2.2. Structural, morphological and chemical characterization of Sn–Co NWs

Structural characterization of the samples was performed by X-ray diffraction with a PW 1130 Philips generator working with Cu Kα radiation ($\lambda = 1.54$ Å) and a PW 1050 goniometer. Morphological features were determined by a field emission gun – environmental scanning electron microscope (FEG-ESEM, FEI Quanta™ 200F) equipped with an X-ray energy dispersive spectrometer (EDS), which was used to determine the composition of the Sn–Co NWs. The total Sn–Co mass was evaluated by a ME36S Sartorius Mechatronics microbalance.

2.3. Electrochemical characterization of Sn–Co NWs

The deposited Sn–Co NWs with a Sn load in the range of 0.4–0.6 mg cm^{-2} were cut in several disks of 0.61 cm^2 geometric area. The disks were assembled in Swagelok-type cells in an argon-filled Mbraun Labmaster 130 dry-box (H_2O and $O_2 < 1$ ppm). The NW electrode was separated from the counter electrode by a glass separator (Whatman GF/D 400 μm thick) soaked in the same electrolyte as the cell's, which was EC:DMC 1:1-$LiPF_6$ 1 M (LP30, Merck) with 5 wt. % vinylene carbonate (VC, 97%, Fluka) as additive when indicated. Lithium foils were used for half-cell tests as both reference and counter electrodes and the cells were first tested by five galvanostatic charge-discharge cycles at 0.075 mA (which corresponds to a C-rate ranging from C/3 to C/5 depending on the electrode loading) and at different C-rate for the following cycles with potential cut-offs of 0.02 and 2.00 V *vs.* Li. The Sn–Co NW electrode was assembled for tests in battery configuration against $LiFePO_4$ and a lithium foil was used as reference electrode. The Sn–Co NW electrodes were pre-cycled (ca. 10 cycles) before their assembling in battery in order to reach an almost stable coulombic efficiency value. The cathode was prepared via a slurry composed of 90 wt. %. $LiFePO_4 \cdot V_2O_3$ (Advanced Lithium Electrochemisty Co., Ltd.), 5 wt. % carbon Super P (Erachem Comilog) as conducting additive and 5 wt. % PVdF (Kynar HSV 900, Arkema) as binder. The slurry was spread onto an etched Al foil (15 μm thick) and dried at 60 °C until the complete solvent evaporation and then at 120 °C for 2 h. Finally, 9 mm diameter disks were cut, pressed (3000 psi for 3 min) and dried at 150 °C under dynamic vacuum (10^{-3} torr). Galvanostatic charge-discharge cycles were carried out at C/2 with potential cut-offs of 4.0 and 1.0 V for the battery, and 4.3 V and 0.02 V *vs.* Li for the charge of $LiFePO_4$ cathode and Sn–Co NW anode, respectively. All the electrochemical characterizations were performed by a Perkin–Elmer VMP multichannel potentiostat/galvanostat at 30° and 10 °C.

3. Results and discussion

In Fig. 1 the XRD spectrum of a typically deposited Sn–Co NWs displays intense peaks assigned to the copper current collector and no reflection peak attributable to the Sn or Sn–Co alloy, thereby demonstrating that such an electrodeposited Sn–Co alloy is amorphous. Fig. 2 shows the SEM images of the Sn–Co nanowires: they have a diameter of 300 nm and a length of 6 μm. The randomly interconnected NWs are well distributed over the entire surface of the current collector and have significant elbowroom to accommodate volume expansion during lithium insertion. Fig. 3 shows the EDS spectrum with the corresponding element mass and atomic percentages of a top view of a Sn–Co NW electrode which demonstrates that the tin content in the binary amorphous Sn–Co alloy is 59 wt. %, corresponding to the Sn_2Co_3 alloy. In our previous paper the tin content of the amorphous alloy was 87 wt. % [5]. For

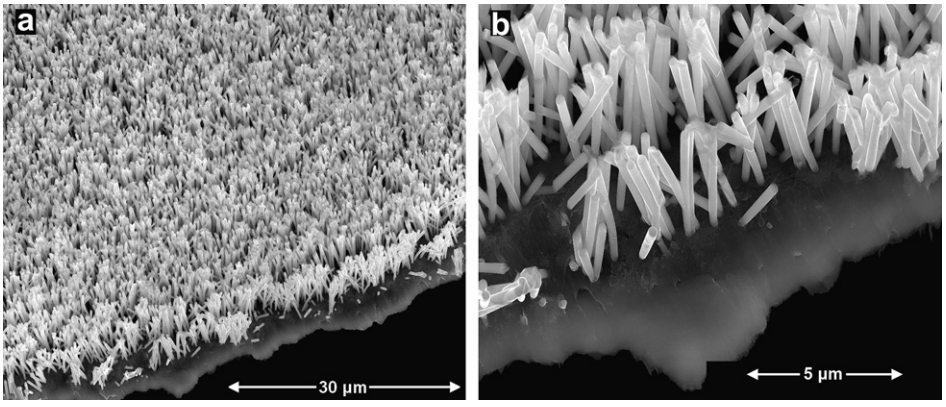

Fig. 2. SEM images of Sn–Co NW array over copper current collector. (a) Overall view, (b) detail of the contact between Sn–Co NWs and copper current collector.

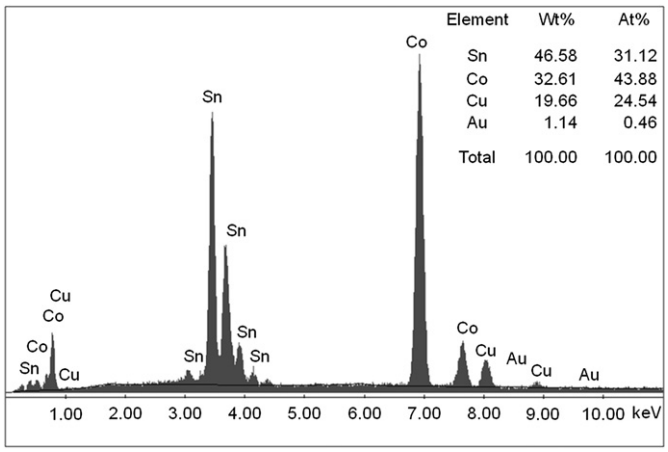

Fig. 3. EDS spectrum with the corresponding element mass and atomic percentages of a Sn–Co NW electrode top view.

the increase of the Co content (from 13 wt. % to 41 wt. %) both the decrease of the Sn^{2+}/Co^{2+} molar ratio in the electrolytic bath and the shift of the deposition potential from −1.0 to −1.3 V *vs.* SCE played a relevant role.

Fig. 4 displays the charge-discharge voltage profiles of representative cycles of a Sn_2Co_3 NW electrode tested by 200 deep galvanostatic cycles between 0.02 and 2.00 V *vs.* Li at C/2-rate and 30 °C. Fig. 5 reports the corresponding capacity per cm^2 (geometric area) and the coulombic efficiency *vs.* cycle number. The electrode delivered ca. 0.40 mAh cm^{-2} over 150 cycles: there was no significant capacity fade over 100 cycles and a 20% fade after 200 cycles, and the specific capacity referred to the tin mass approached the theoretical value (993 mAh g^{-1}) over more than 100 cycles. The architecture of these Sn_2Co_3 NWs prevents electrode pulverization as shown in Fig. 6, which displays the SEM image of an electrode after 170 cycles at C/2. The NW structure of the cycled electrode is still evident demonstrating the beneficial effect of the cobalt content increase in the alloy. Like the graphite-based anodes, the Sn_2Co_3 NW electrodes display the formation of a solid electrolyte interface (SEI) evinced by the coulombic efficiency values at the first cycles in the range 75–80%, as shown in Fig. 5. After 40 cycles the efficiency approached an average value of 97%, although this is not high enough to guarantee a long-cycle life for a cell in battery configuration (efficiency values ≥ 99.5% are required).

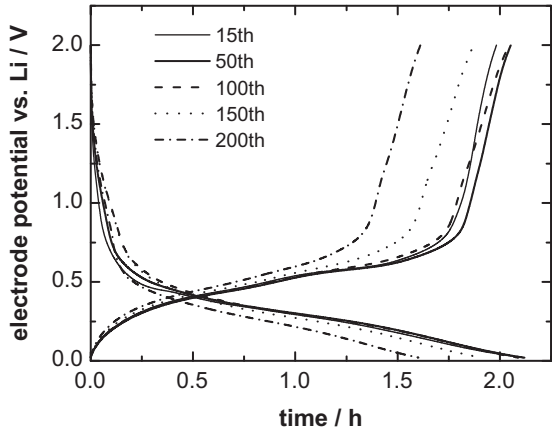

Fig. 4. Voltage profiles of a Sn_2Co_3 NW electrode upon charge-discharge galvanostatic cycles at C/2 (0.126 mA) in EC:DMC 1:1-$LiPF_6$ 1 M at 30 °C.

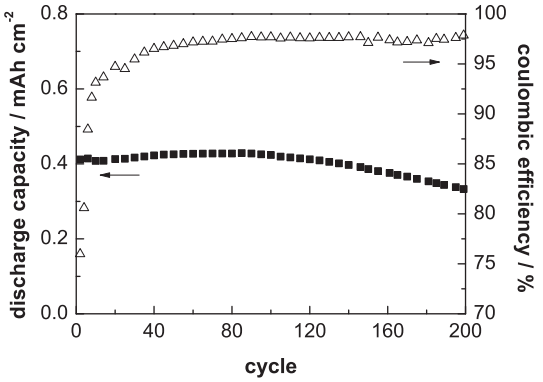

Fig. 5. Discharge capacity (mAh cm^{-2}) and coulombic efficiency *vs.* cycle number of a Sn_2Co_3 NW electrode at C/2 (0.126 mA) in EC:DMC 1:1-$LiPF_6$ 1 M at 30 °C.

Fig. 7 shows the specific capacity of a Sn_2Co_3 NW electrode at different C-rate from C/3 (0.33 A/g of Sn) to 10C (10 A/g of Sn) at 30° and 10 °C. The results evidence the high charge-discharge rate capability of these NW electrodes even at the lowest temperature, as expected for metal based NWs, demonstrating that the Sn_2Co_3 NW electrode is a potential substitute of the graphite anode. This is true taking also in account that with the same membrane design the length of the NWs, and then the Sn mass per geometric area, can be more than doubled by increasing the electrodeposition time.

Batteries with pre-cycled Sn_2Co_3 NW electrodes as anodes (see experimental) and $LiFePO_4$ as cathodes were assembled in three-electrode cells with a Li reference electrode in EC:DMC-$LiPF_6$ electrolyte. The batteries were tested by galvanostatic charge-discharge cycles at 30 °C and C/2 (evaluated on the anode Sn load ranging from 0.47 to 0.61 mg cm^{-2}) between 4.0 and 1.0 V, and with potential cut-offs of 0.02 V and 4.3 V *vs.* Li for the anode and cathode, respectively, during battery charge. Fig. 8 reports the capacity values (Q) normalized to the initial capacity ($Q°$) *vs.* cycle number of these batteries with $Q°$ in the range 0.5–0.6 mAh cm^{-2}. The batteries were assembled with a different ratio (R) of cathode to anode capacity from 1 to 2: battery A featured $R = 1$ and the delivered capacity decreased in a very few cycles, battery B with

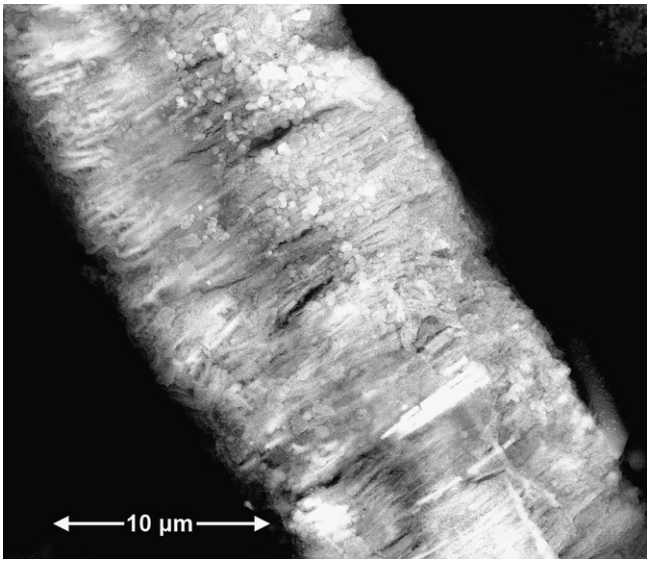

Fig. 6. SEM image of a Sn_2Co_3 NW electrode after 170 cycles at C/2: cross-section view with Cu current collector on the left.

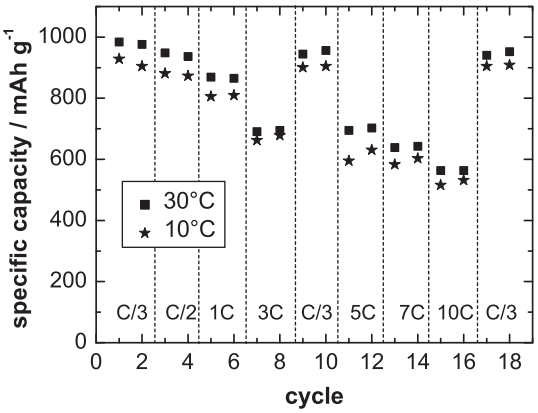

Fig. 7. Discharge specific capacity (mAh g^{-1}) *vs.* cycle number of a Sn_2Co_3 NW electrode in EC:DMC 1:1-$LiPF_6$ 1 M at 30° and 10 °C at different C-rates.

$R = 1.35$ performed 10 cycles before to decline, and battery C with a cathode capacity in excess of 100% ($R = 2$) performed almost 30 stable cycles. The sharp decrease in the performance of all the batteries is attributable to the low efficiency (95–96%) of the Sn_2Co_3 NW electrodes, which prevents over cycling the full lithiation of the cathode that became more and more delithiated reaching the voltage cut-off of 4.3 V. Indeed, battery C, once the $LiFePO_4$ cathode was independently discharged *vs.* Li at C/10 down to 2.2 V, recovered its initial capacity. Fig. 9 displays some representative charge-discharge voltage profiles of the two electrodes for battery C. The first ten cycles (Fig. 9a) exhibit flat voltage profiles for the cathode at ca. 3.4 V *vs.* Li and those for the anode, reaching the cut-off of 0.02 V *vs.* Li, indicate the full lithiation of the electrode. However, the capacity excess of the cathode is rapidly consumed over cycling and from the 28th cycle the cathode voltage profiles move toward the cut-off potential of 4.3 V *vs.* Li during battery charge, leading the battery to its limit potential value of 4.0 V (Fig. 9b). Consequently, the anode does not reach the potentials for a full lithiation and the battery displays a capacity decrease. After independent discharge of the cathode, both the electrodes return as they were at the beginning of cycling (Fig. 9c).

These results indicate the feasible application of these Sn_2Co_3 NWs in battery configuration and to this end a successful SEI-forming additive should be used. Tin-based electrodes undergo large volume changes during lithiation/delithiation, and an SEI

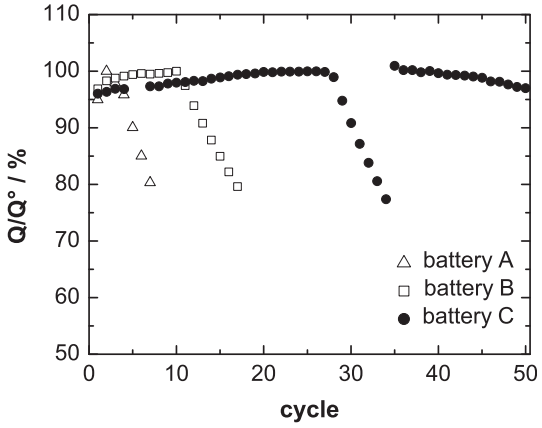

Fig. 8. Normalized capacity Q/Q° (capacity over the initial capacity) *vs.* cycle number of battery A (balanced electrodes), battery B (34% excess of cathode capacity) and battery C (100% excess of cathode capacity) in EC:DMC 1:1-$LiPF_6$ 1 M at 30 °C.

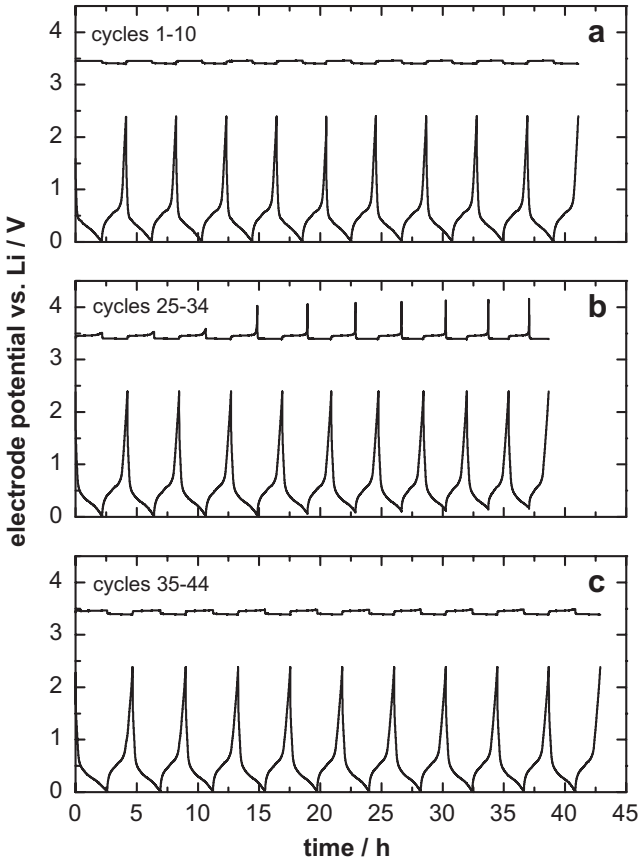

Fig. 9. Charge-discharge voltage profiles of the $LiFePO_4$ cathode (thin line) and the Sn_2Co_3 NW anode (thick line) of the battery C at C/2 in EC:DMC 1:1-$LiPF_6$ 1 M at 30 °C.

with good mechanical properties should reflect positively on cycling efficiency. The addition of VC in the electrolyte greatly improves the graphite electrode performance [10] and we used this additive even for Sn_2Co_3 NW electrodes. Fig. 10 shows the capacity and coulombic efficiency values *vs.* cycle number of a Sn_2Co_3 NW electrode tested with 5 wt. % VC by galvanostatic cycles between 0.02 V and 2.00 V *vs.* Li at C/2 and 30 °C. The tin loading of this electrode was higher compared to that of the electrode reported in Fig. 5 and delivered a very stable capacity of 0.6 mAh cm^{-2} over 100 cycles. The efficiency value at the first cycle in the VC-containing electrolyte was 75% and reached an average efficiency value of

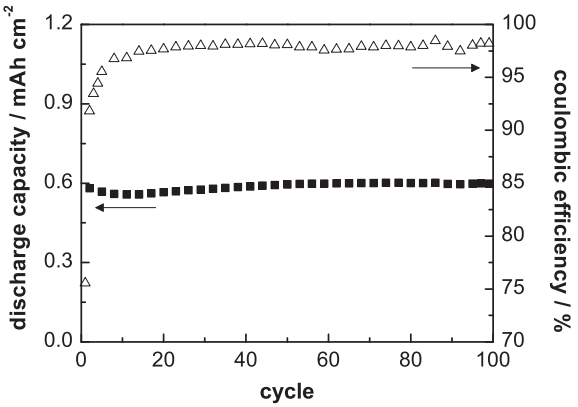

Fig. 10. Discharge capacity (mAh cm^{-2}) and coulombic efficiency *vs.* cycle number of Sn_2Co_3 NW electrode in EC:DMC 1:1-$LiPF_6$ 1 M – 5% VC at 30 °C.

98% after 20 cycles. The VC additive in the electrolyte improved the efficiency, but the values are still low for long-cycle life batteries and new additives should be tested.

4. Conclusions

The high cobalt content in the Sn_2Co_3 alloy NWs yielded electrodes with good mechanical stability over cycling in half-cell *vs.* Li. Sn_2Co_3 NW electrodes performed 200 deep galvanostatic charge-discharge cycles with a capacity retention of 80%, a coulombic efficiency approaching 97% after 40 cycles and delivering up to 0.6 mAh cm^{-2} when the NWs were 6 μm long. Furthermore, the high charge-discharge rate capability of the Sn_2Co_3 NW electrodes even at 10 °C make them attractive as anode in lithium-ion batteries, also in consideration that with the same membrane the mass of the tin per geometric area can be more than doubled. The feasible application of these electrodes in battery configuration against $LiFePO_4$ has been demonstrated and the results suggest that efforts should be focused on the selection of electrolyte additives to enhance over 99.5% the coulombic efficiency of the charge-discharge cycles of the Sn_2Co_3 NWs. The VC additive used improved the coulombic efficiency but not enough for long-cycle life cells in battery configuration.

Acknowledgments

The authors would like to thank CR Mobility Solution System S.r.l. for the financial support.

References

[1] M. Winter, J.O. Besenhard, Electrochim. Acta 45 (1999) 31.
[2] J.R. Dahn, R.E. Mar, A. Abouzeid, J. Electrochem. Soc. 153 (2006) A361.
[3] N. Li, C.R. Martin, J. Electrochem. Soc. 148 (2001) A164.
[4] X. Zhao, Z. Xia, D. Xia, Electrochim. Acta 55 (2010) 6004.
[5] G. Ferrara, L. Damen, C. Arbizzani, R. Inguanta, S. Piazza, C. Sunseri, M. Mastragostino, J. Power Sources 196 (2011) 1469.
[6] Z. Du, S. Zhang, J. Phys. Chem. C 115 (2011) 23603.
[7] J. Wang, N. Du, H. Zhang, J. Yu, D. Yang, J. Phys. Chem. C 115 (2011) 23620.
[8] M. Tian, W. Wang, S.-H. Lee, Y.-C. Lee, R. Yang, J. Power Sources 196 (2011) 10207.
[9] J. Chen, L. Yang, S. Fang, S.-i. Hirano, K. Tachibana, J. Power Sources 199 (2012) 341.
[10] S.S. Zhang, J. Power Sources 162 (2006) 1379.